NANO LETTERS

2006
Vol. 6, No. 9
2060−2065

Localized Surface Plasmon Resonance Spectroscopy of Single Silver Triangular Nanoprisms

Leif J. Sherry, Rongchao Jin, Chad A. Mirkin, George C. Schatz,* and Richard P. Van Duyne*

Chemistry Department, Northwestern University, 2145 Sheridan Road, Evanston, Illinois 60208-3113

Received June 5, 2006

ABSTRACT

The plasmonic properties of single silver triangular nanoprisms are investigated using dark-field optical microscopy and spectroscopy. Two distinct localized surface plasmon resonances (LSPR) are observed. These are assigned as in-plane dipolar and quadrupolar plasmon excitations using electrodynamic modeling based on the discrete dipole approximation (DDA). The dipole resonance is found to be very intense, and its peak wavelength is extremely sensitive to the height, edge length, and tip sharpness of the triangular nanoprism. In contrast, the intensity of the quadrupole resonance is much weaker relative to the dipole resonance in the single particle spectra than in the ensemble averaged spectrum. Several parameters relevant to the chemical sensing properties of these nanoprisms have been measured. The dependence of the dipole plasmon resonance on the refractive index of the external medium is found to be as high as 205 nm RIU^{-1} and the plasmon line width as narrow as ∼0.17 eV. These data lead to a sensing figure of merit (FOM), the slope of refractive index sensitivity in eV RIU^{-1}/line width (eV), as high as 3.3. In addition, the LSPR shift response to alkanethiol chain length was found to be linear with a slope of 4.4 nm per CH_2 unit. This is the highest short-range refractive index sensitivity yet measured for a nanoparticle.

Significant attention has been given to the study of the plasmonic properties of noble metal nanoparticles as a result of their potential uses as components in a diverse range of technologies such as waveguides,[1−3] photonic circuits,[4,5] molecular rulers,[6] and chemical/biological sensors.[7−10] All of these applications are based on the localized surface plasmon resonance (LSPR) of the nanoparticle. LSPRs are excited when electromagnetic radiation interacts with a nanoparticle to create coherent oscillations (excitations) of the conduction electrons. This phenomenon has two key consequences: (1) selective photon absorption and scattering allows the optical properties of the nanoparticles to be monitored by conventional UV−vis spectroscopy and far-field scattering techniques and (2) enhancement of the electromagnetic fields surrounding the nanoparticles lead to surface-enhanced spectroscopic techniques including surface-enhanced Raman spectroscopy. Previous studies show that the plasmon frequency is extremely sensitive to nanoparticle composition,[11] size,[12] shape,[13−15] dielectric environment,[9,10,16−18] and proximity to other nanoparticles.[19−22] The Van Duyne and Halas groups have demonstrated the ability to tune the plasmon frequency of nanoparticles across the visible and near-IR spectra.[12,23] Another feature of interest is the observation of multiple plasmon peaks in the far-field Rayleigh LSPR spectra of nanorods,[24−26] triangular nanoprisms,[13] and nanocubes.[16] These are caused either by multipolar excitation or by interaction with the surroundings, such as with an asymmetric dielectric environment or with other nearby metal particles.

With such a wide range of tunable parameters, spectral signatures, and sensitivity to their "nanoenvironments", nanoparticles have become good platforms for pursuing high throughput, small volume, low-cost, ultrasensitive, multiplexed chemical/biological sensors.[27] However, most of these applications are based on ensemble-averaged spectral properties.[7,8,28] To date five different ensemble averaged nanoparticle sensing mechanisms have been demonstrated. These are (1) surface-enhanced Raman scattering,[29−31] (2) local refractive index changes,[8,9,17,32,33] (3) charge-transfer interactions at nanoparticle surfaces,[34,35] (4) resonant Rayleigh scattering from nanoparticles used as labels,[36−38] and (5) nanoparticle aggregation.[39−42]

To better understand the design rules for practical plasmonic sensing devices, the properties of single nanoparticles, including the relationship between particle morphology, plasmon spectral position (λ_{max}), dielectric sensitivity, and sensing volume, need to be understood in greater detail. Recent theoretical work by Lazarides and co-workers has suggested that nanoparticle dielectric sensitivity is independent of nanoparticle morphology.[43] Instead they suggest that

* Corresponding authors: Richard P. Van Duyne, vanduyne@chem.northwestern.edu, telephone (847) 491-3516, fax (847) 491-7713; George C. Schatz, schatz@chem.northwestern.edu, telephone (847) 491-7713.

10.1021/nl061286u CCC: $33.50
Published on Web 07/27/2006

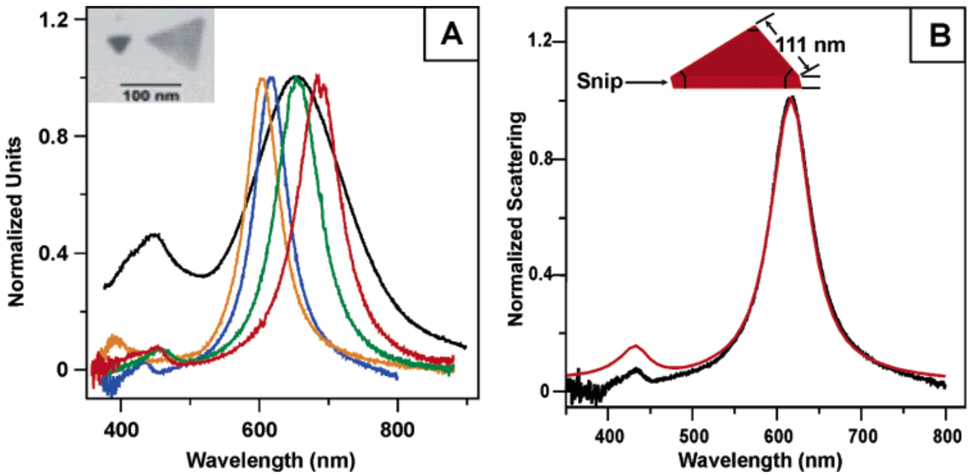

Figure 1. LSPR spectra of silver triangular nanoprisms: (A) ensemble extinction spectrum (black curve) vs single nanoparticle dark-field scattering spectra (colored curves) of triangular nanoprisms (representative nanoprisms shown in TEM inset); (B) theoretical modeling (red curve) of a single triangular nanoprism using the DDA method. The theoretical spectrum was calculated for a nanoprism with edge length = 111 nm, snip = 15 nm, and height = 10 nm.

it is only the spectral position of the plasmon that determines the dielectric sensitivity of a nanoparticle. A caveat to this assertion is that this will be true only when the particle is in a homogeneous dielectric environment. This is critical since many measurements on nanoparticles are performed in an inhomogeneous dielectric environment (e.g., particles on surfaces or particles that are chemically functionalized in an asymmetric manner).

These issues are addressed here by studying the LSPR spectroscopy and dielectric sensitivities of single silver triangular nanoprisms. This is done by immersing the nanoparticles in a variety of bulk dielectric environments as well as by modifying their surfaces with straight-chain alkanethiols to create nanoenvironments. Although there have been previous studies on triangular nanoprisms,[13,15] the present studies are the first for single nanoparticles. It will be important to see how the results compare, as much of the interpretation of the nanoparticle spectra have involved comparing ensemble averaged results with theory done for single nanoparticles. These earlier comparisons have provided significant information about the nanoparticle properties, including the assignment of the modes of plasmon excitation which are responsible for each of the three experimentally observed plasmon peaks.[13] They also have demonstrated the exceptional degree of tunability which this structure allows through changes in height, width, and tip sharpness.[15] By judiciously selecting nanoprisms with one or more plasmon modes that have the same λ_{max}, three of the four nanoparticle observables mentioned previously (λ_{max}, dielectric sensitivity, and sensing volume) are able to be investigated at the single particle level.

The nanoprisms studied in this work were synthesized by the Mirkin method (both with and without bis(*p*-sulfonatophenyl)phenylphosphine (BSPP) surfactant) whereby small spherical seed nanoparticles ~15 nm in diameter are used as precursors in an optically driven mechanism of triangular nanoprism growth.[13] Ensemble extinction measurements were acquired in solution using standard UV−vis transmission spectroscopy. In addition, single nanoprism scattering measurements were determined by resonant Rayleigh dark-field optical microscopy as described elsewhere.[9,16] Samples were prepared by drop coating approximately 2 μL of the nanoprism solution on a no. 1 glass coverslip in order to immobilize the nanoprisms as the solvent evaporates from the substrate surface in an inert nitrogen gas environment. This volume of the nanoprism solution proved optimal for yielding a density of nanoparticles on the glass substrate surface that allowed for multiple nanoprisms to be viewed simultaneously using wide-field optical microscopy while maintaining sufficient spatial separation so as to avoid electromagnetic coupling between the nanoparticles. In addition to these measurements, finite element electrodynamics calculations were performed to characterize the spectra of the nanoparticles using the discrete dipole approximation (DDA)[44] where the nanoprism was represented by 48 000 dipoles, which yielded a dipole grid length of 1 nm. This method has been successfully used in many past studies of nanoparticle optical properties,[14,26,45,46] and the only major complication in the present calculation arises in the modeling of substrate effects, where the effective medium approach that was described by Malinsky et al. has been used.[47]

Figure 1 compares triangular nanoprism LSPR spectra from three different sources: transmission UV−vis spectroscopy (ensemble of nanoprisms in solution), resonant Rayleigh scattering spectroscopy (single nanoprism), and DDA calculations (single nanoprism). The prisms in these samples were made using BSPP. Figure 1A compares the ensemble extinction spectrum (scattering + absorption) of an aqueous solution (refractive index = 1.33) of nanoprisms to the spectra of four different single nanoprisms that are also immersed in an aqueous environment. These single nanoprism scattering spectra illustrate the degree of geometric diversity contained in a given aliquot of a nanoprism solution. The inset is a transmission electron microscopy (TEM) image of nanoprisms taken from the aqueous solution, but these prisms are not the specific nanoprisms responsible for any of the depicted spectra. Figure 1B compares the spectrum

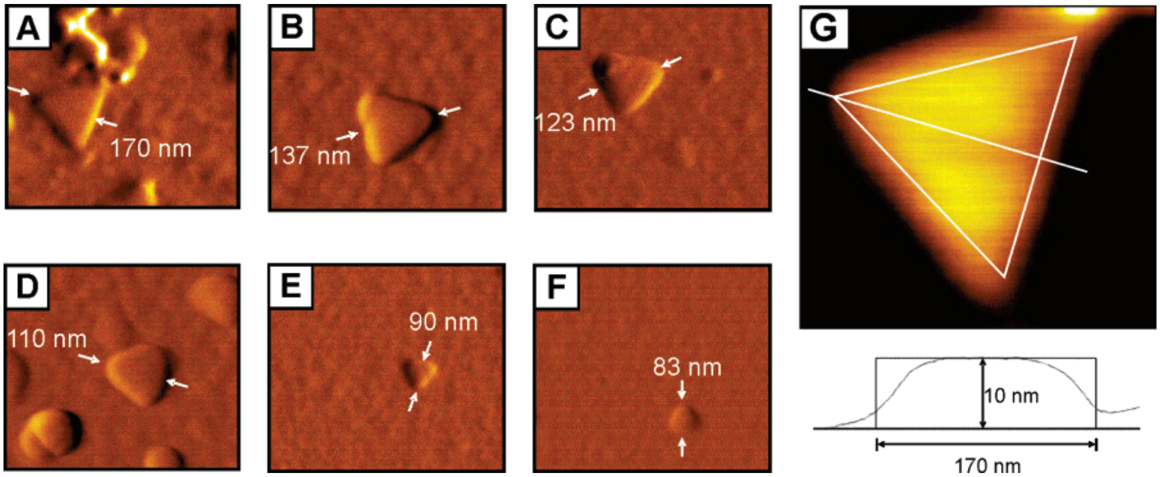

Figure 2. (A−F) AFM measurements showing the diversity found in a typical 2 μL triangular nanoprism aliquot. (G) Height cross section for the nanoprism shown in (A).

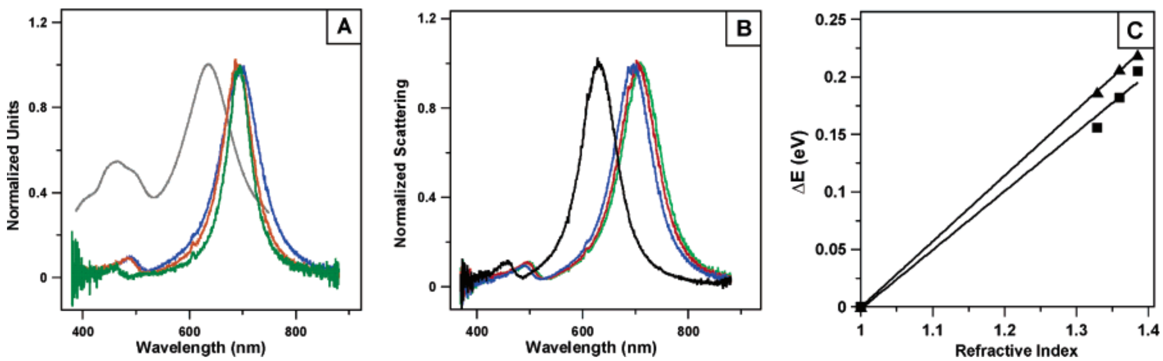

Figure 3. (A) Ensemble extinction spectrum (gray curve) vs single nanoparticle LSPR scattering spectra of silver triangular nanoprisms synthesized without surfactant. (B) Single nanoprism dark-field scattering spectra in four different dielectric environments (refractive indexes = 1.000297, 1.329, 1.359, 1.383) demonstrating the nanorism's sensitivity to its environment. (C) Linear regression fit to the experimental data. Triangles represent dipole data (m = 0.571 eV RIU^{-1}, R^2 = 0.999,) and squares represent quadrupole data (m = 0.512 eV RIU^{-1}, R^2 = 0.992).

of a single nanoprism acquired in an inert nitrogen environment (refractive index = 1.000297) with a nanoprism spectrum calculated with the DDA method.[44] This spectrum shows typical behavior for a prism[13] in which there is a strong dipole resonance at 620 nm, and then a weaker in-plane quadrupole resonance at 433 nm. A third plasmon resonance, due to out-of-plane quadrupole excitation, which has previously been noted at 325 nm, is not accessible in our measurements. The particle structure parameters used to calculate this spectrum were not exactly from physical measurements of the nanoprism yielding the experimental spectrum. Instead, the geometric parameters used in the calculation in Figure 1B were allowed to vary until the experimental result was sufficiently reproduced. Atomic force microscopy (AFM) measurements on several different nanoprisms, shown in Figure 2, reveal that the geometric parameters used to model the experiment fall well within the range of measured values. These images explicitly show the lack of geometric homogeneity in the nanoprism samples, in particular the variation in edge length and tip sharpness.

Figure 3 shows LSPR spectra of nanoprisms synthesized without the use of the BSPP surfactant. This was done since it was discovered that straight-chain alkanethiols do not displace the surfactant, making it difficult to functionalize the BSPP-coated particles for sensing applications. Figure 3A compares the ensemble extinction LSPR spectrum to three single LSPR scattering spectra. As one can see, the ensemble averaged spectra show considerably less homogeneity in the line shape of the in-plane quadrupole peak at ~465 nm, reflecting the contribution of particles in the sample that are not nanoprisms. The single nanoprism spectra displayed in Figure 3A have been deliberately chosen to have overlapping in-plane dipole LSPR peak positions so as to address the relative importance of geometry vs plasmon resonance position in nanoparticle refractive index sensitivity.

Figure 3B shows a single nanoprism from Figure 3A (blue curve) in a variety of different bulk dielectric environments. It should be noted that prior to all our experimental measurements the nanoparticles were solvent annealed by incubating the nanoprisms in ethanol for at least 12 h. This is necessary since nanoparticles can undergo geometrical changes when initially exposed to a solvent environment.[17] After the annealing process, LSPR spectra of the nanoprisms were acquired in nitrogen after brief incubations (~10 min) in methanol, ethanol, and 1-propanol; this assured us that the LSPR spectrum would not suffer any additional shifts due to further solvent annealing. Once the geometric integrity of the nanoprisms is established, their refractive index

Table 1. Peak Positions and Pertinent Experimental Environmental Sensitivity Parameters for the Dipole Resonance of Three Different Nanoprisms with Approximately Equal Dipole λ_{max}

	dipole λ_{max} (nm)	dipole sensitivity (nm/RI units)	dipole sensitivity (meV/RI units)	fwhm (meV)	FOM
nanoprism 1	630.6	204.9	571.1	246.3	2.319
nanoprism 2	634.6	182.9	511.4	195.3	2.619
nanoprism 3	631.4	196.4	549.1	165.8	3.294

Table 2. Peak Positions and Pertinent Experimental Environmental Sensitivity Parameters for the Quadrupole Resonance of Three Different Nanoprisms with Approximately Equal Dipole λ_{max}

	quad λ_{max} (nm)	quad sensitivity (nm/RI units)	quad sensitivity (meV/RI units)	fwhm (meV)	FOM
nanoprism 1	459.3	93.99	511.6	284.1	1.801
nanoprism 2	460.8	80.64	440.8	267.5	1.648
nanoprism 3	439.6	78.62	481.8	166.7	2.890

Table 3. LSPR λ_{max} Shift Data Acquired after Surface Modification with Decanethiol for Three Different Nanoprisms with Approximately Equal Dipole λ_{max}

	fwhm (meV)	dipole shift (nm)	dipole shift (meV)	reference shift (meV)	% reference shift (meV)	quad shift (nm)	quad shift (meV)
nanoprism 1	246.3	19.84	59.96	71.15	84.27	16.81	96.10
nanoprism 2	195.3	11.56	34.97	71.15	49.15	4.44	25.46
nanoprism 3	165.8	14.69	46.80	71.15	65.78	6.14	38.83

sensitivity is measured (parts B and C of Figure 3). These data show that the nanoprisms' dipole and quadrupole plasmon resonances respond linearly to changes in the refractive index of their environment and that the dipole's response is stronger than the quadrupole's.

Tables 1 and 2 list the peak position, refractive index sensitivity, plasmon line width fwhm, and figure of merit (FOM) for each of the three single nanoprisms in Figure 3A. The FOM,[16] which is defined using

$$\mathrm{FOM} = \frac{m(\mathrm{eV\ RIU}^{-1})}{\mathrm{fwhm\ (eV)}} \qquad (1)$$

functions as a standard measure for assessing a nanoparticle's sensing potential. The results show that the bulk refractive index sensitivities of nanoprisms vary significantly (~11%) despite overlapping dipole λ_{max}'s (at most a 0.6% change in dipole LSPR peak position). This demonstrates that the Lazarides argument is not valid (as expected) when a nanoparticle is in an inhomogeneous dielectric environment (nanoparticles on a glass substrate).

The results in Tables 2 and 3 provide an important opportunity to study the influence of plasmon width on particle structure. Previous experimental and theoretical studies have demonstrated the sensitivity of λ_{max} to changes in particle geometry (i.e., edge length, thickness, and tip sharpness),[13,14] and the present results are consistent with past expectations. However the variation of the plasmon line width with changes in nanoprism structure, holding λ_{max} constant, has not been studied even though this is an important component of the FOM. The data in Tables 2 and 3 demonstrate substantial variation in the plasmon width, and this plays an important role in determining the FOM. The absence of information about particle structure in these measurements limits our ability to explain what factors are important in determining this behavior; however the DDA calculations can be used to provide qualitative insight.

Previous studies have shown that there are two distinct regimes (intrinsic and extrinsic) of the plasmon bandwidth for high symmetry (spheres, rods, etc.) noble metal nanoparticles.[24,48] The intrinsic regime applies to nanoparticles with radii smaller than their mean free electron path. In this regime, the surface of the nanoparticle becomes the dominant scattering source for the conduction electrons and thereby determines the lifetime of the excited electrons. Smaller radii lead to shorter lifetimes and, hence, larger bandwidths. The DDA calculations have not included the intrinsic effect; however we note that the good agreement between theory and experiment in Figure 1B suggests that this must not be very important for the particle sizes studied here.

The extrinsic regime applies to nanoparticles with radii larger than their mean free electron path. In this regime, electron−electron, electron−phonon, and electron defect scattering dominate, which are contributions that should be size independent. However, broadening of the plasmon bandwidth with increasing particle size does occur as a result of radiative damping. This arises when the induced dipole in the particle emits light at a rate that competes with the rate of excitation of the particle. For spherical particles this effect scales with the square of the volume of the particle, and it becomes important for particles with diameters larger than 100 nm. In the case of the nanoprisms, our DDA calculations show that the bandwidth does not increase with increasing edge length (considering edges in the 80−200 nm range) or with particle height (for 8−15 nm heights). This is consistent with the idea that the particle volume is too small for radiative damping to be important.

However, our DDA calculations show that there is one structure that is important in determining the LSPR width, the sharpness of the tips of the particles: i.e., the sharper the tips the broader the line width. Since we are comparing results for fixed λ_{max}, the particle tip sharpness is controlled by "snipping" the tips (and readjusting particle size), and

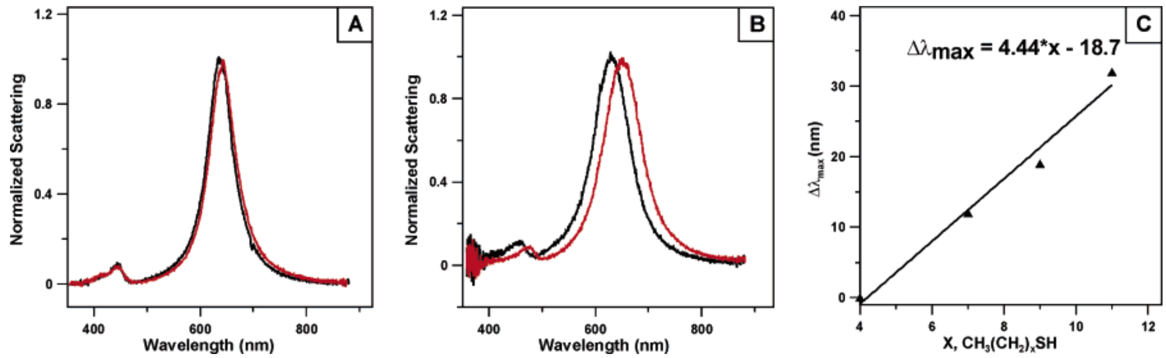

Figure 4. LSPR dark-field scattering specta of single silver nanoprisms before (black) and after (red) surface modification with (A) 1-hexadecanethiol (5 nm dipole shift; BSPP capped) and (B) 1-decanethiol (19.84 nm shift; citrate capped). (C) Plot depicting the linear relationship between the LSPR response and the SAM alkyl chain length.

the broadest resonances are obtained by unsnipped (perfectly sharp) tips. Physically the coupling of tip sharpness to plasmon width is a manifestation of the well-known lightning rod effect, and it also can be understood in terms of roughness-induced momentum matching of surface plasmons to the radiation field.

Although the DDA results provide a straightforward mechanism for understanding the width data in Tables 1 and 2, we are not able to perform a quantitative assessment of this interpretation due to the lack of measured structural information about the specific particles being considered. We do note, however, that theory and experiment yield good qualitative agreement for the variation in the observed plasmon line widths. Our calculations show that up to ∼41% variation in line width is expected for particles with between 0 and 18% of their tips snipped. The experimental data show up to ∼33% variation. It is expected for theory to show a larger variation in line width since it can represent nanoprisms with perfectly sharp tips, while the tips of the chemically synthesized nanoprisms are never perfectly sharp. Also, we cannot rule out the variation of particle dielectric constant with internal structure of the particles (twinned crystal planes, crystal defects, etc.) might provide an alternative mechanism for the observed line widths. Current experiments are aimed at exploring the relative importance of these two causes.

We now turn to the refractive index sensing properties of single silver nanoprisms. Parts A and B of Figure 4 show the LSPR spectra of two different nanoprisms before and after a 1 h incubation in alkanethiol (Sigma Aldrich) solution. The nanoprism in Figure 4A was synthesized with the surfactant BSPP as the capping agent and was incubated in 1-hexadecanethiol. The nanoprism in Figure 4B was synthesized with citrate as the capping agent and was incubated in 1-decanethiol. These data show that BSPP is not, and citrate is displaced by the binding of thiol molecules to the nanoprism surface. This fact is important since the use of BSPP allows for improved control of nanoprism synthesis (higher yield, better size homogeneity, and sharper tips),[13] which is critical for optimizing the sensing properties of single nanoparticles. This can be seen in Figure 4C, which shows the relationship between alkanethiol chain length and the maximum observed LSPR shift. By control of the shape of the nanoparticles, the increment in wavelength per CH_2 group is 1 nm larger in the present measurements (4.44 nm per CH_2 group vs 3.5 nm per CH_2 group) than with previously studied citrate reduced single nanoparticles (involving randomly selected particles) for the dipole plasmon resonance.[9]

Table 3 lists the LSPR shift data due to adsorption of 1-decanethiol to the surface of the three single nanoprisms shown in Figure 3 for both their dipole and quadrupole resonances. The reference shift in Table 3 is based on previous experimental work by Van Duyne and co-workers on triangular truncated tetrahedra (120 nm perpendicular bisector and 50 nm height) modified with 1-decanethiol.[17] Note that the nanoprism with the greatest line width experiences the largest shift upon chemical modification. If we assume that line width correlates with tip sharpness as described above, then we can also understand why this also leads to the largest shift upon chemical modification. This is because earlier theory from Schatz and co-workers has demonstrated that the dielectric shift is largest where the near-field is largest,[46] and the near-field is largest for the sharpest tips. The other two nanoprims do not obviously follow this argument since nanoprism 3 (narrower line width) experiences a greater shift than nanoprism 2. However other factors can make the shift associated with molecules that coat the entire surface of the particle scale differently than that associated with just the tip regions.[45,46,49]

Note that there are no reference shift data for the quadrupole peak since this is, to our knowledge, the first time a quadrupole plasmon resonance has been shown to respond to local refractive index changes. The quadrupole excitation of a nanoprism yields broader plasmon resonances, less sensitivity to bulk and local refractive index changes, and lower FOM values relative to the dipole excitation.The only deviation from these trends was observed for the shift induced by 1-decanethiol bound to the surface of nanoprism one. In this case the quadrupole shift was greater (in energy units) than the dipole shift.

Single nanoprisms show great promise as chemical and biological sensors for three reasons: (1) The single nanoprisms studied are approximately five times thinner than the nanoparticles used in the comparison data set. This implies that the electromagnetic fields of the nanoprisms extend significantly farther from their surface than those of the reference particles since it was shown by Van Duyne and co-workers that thinner particles have larger sensing volumes.[45,49] Hence, the shifts recorded for the nanoprisms are due to a much lower percentage of the total sensing volume than was the case for the reference particles. (2) Virtually all the nanoprisms in a given sample have some amount of tip snipping (average ~10−15% of the unsnipped edge length). If we restrict our measurements to particles with sharper tips, then larger refractive index sensitivity can be achieved since most of triangular nanoparticle's near-field electromagnetic enhancement is localized to the particle's sharp tips.[46] (3) All triangular prism spectra blue shift when first exposed to solvent. This is generally interpreted as further annealing of a prism's sharp tips. If the tips can be protected, nanoprism sensing performance will be improved. Strategies to protect the nanoprisms are currently being developed.

In summary, the plasmonic properties of *single* silver nanoprisms have been studied for the first time and shown to be superior to comparable ensemble averaged nanoparticle plasmonic sensors. It is evident that geometric parameters, along with plasmon position, play a key role in the sensitivity of the nanoprisms to both bulk (solvent) and local (surface chemical modification) refractive index changes. This agrees with previous statements on the subject, and an approach to more carefully explore this issue is being developed. While sensitivities to chemical binding varied from 50 to 85% of that observed for ensemble triangular structures (truncated triangular tetrahedra),[17] it should be noted that these nanoprisms are ~5× thinner than the truncated tetrahedra. Hence, the nanoprisms should be even better for sensing of large biomolecules since these will fill a greater percentage of a nanoprism's sensing volume. Finally, measurement of a nanoparticle's quadrupole plasmon response to changes in the local refractive index has been demonstrated for the first time. Hence, this information provides an experimental probe of the LSPR quadrupolar fields surrounding a nanoparticle, and in some cases it provides greater sensitivity to adsorbates than do dipole resonances.

Acknowledgment. This work was supported by the National Science Foundation (EEC-0118025, CHE-0414554, BES-0507036) and the Air Force Office of Scientific Research MURI program (F49620-02-1-0381). The authors thank Erin M. Hicks for the TEM images in Figure 1.

References

(1) Smolyaninov, I. I.; Hung, Y.-J.; Davis, C. C. *Appl. Phys. Lett.* **2005**, *87*, 241106/1.
(2) Maier, S. A.; Kik, P. G.; Atwater, H. A.; Meltzer, S.; Harel, E.; Koel, B. E.; Requicha, A. A. G. *Nat. Mater.* **2003**, *2*, 229.
(3) Krenn, J. R. *Nat. Mater.* **2003**, *2*, 210.
(4) Ozbay, E. *Science* **2006**, *311*, 189.
(5) Vasseur, J. O.; Akjouj, A.; Dobrzynski, L.; Djafari-Rouhani, B.; El Boudouti, E. H. *Surf. Sci. Rep.* **2004**, *54*, 1.
(6) Reinhard, B. M.; Siu, M.; Agarwal, H.; Alivisatos, A. P.; Liphardt, J. *Nano Lett.* **2005**, *5*, 2246.
(7) Elghanian, R.; Storhoff, J. J.; Mucic, R. C.; Letsinger, R. L.; Mirkin, C. A. *Science* **1997**, *277*, 1078.
(8) Haes Amanda, J.; Chang, L.; Klein William, L.; Van Duyne Richard, P. *J. Am. Chem. Soc.* **2005**, *127*, 2264.
(9) McFarland, A. D.; Van Duyne, R. P. *Nano Lett.* **2003**, *3*, 1057.
(10) Mock, J. J.; Smith, D. R.; Schultz, S. *Nano Lett.* **2003**, *3*, 485.
(11) Link, S.; Wang, Z. L.; El-Sayed, M. A. *J. Phys. Chem. B* **1999**, *103*, 3529.
(12) Haynes, C. L.; Van Duyne, R. P. *J. Phys. Chem. B* **2001**, *105*, 5599.
(13) Jin, R.; Cao, Y.; Mirkin, C. A.; Kelly, K. L.; Schatz, G. C.; Zheng, J. G. *Science* **2001**, *294*, 1901.
(14) Kelly, K. L.; Coronado, E.; Zhao, L. L.; Schatz, G. C. *J. Phys. Chem. B* **2003**, *107*, 668.
(15) Jin, R.; Cao, Y. C.; Hao, E.; Metraux, G. S.; Schatz, G. C.; Mirkin, C. A. *Nature (London)* **2003**, *425*, 487.
(16) Sherry, L. J.; Chang, S.-H.; Schatz, G. C.; Van Duyne, R. P.; Wiley, B. J.; Xia, Y. *Nano Lett.* **2005**, *5*, 2034.
(17) Malinsky, M. D.; Kelly, K. L.; Schatz, G. C.; Van Duyne, R. P. *J. Am. Chem. Soc.* **2001**, *123*, 1471.
(18) Xu, G.; Chen, Y.; Tazawa, M.; Jin, P. *J. Phys. Chem. B* **2006**, *110*, 2051.
(19) Huang, W.; Qian, W.; El-Sayed, M. A. *J. Phys. Chem. B* **2005**, *109*, 18881.
(20) Zhao, L.; Kelly, K. L.; Schatz, G. C. *J. Phys. Chem. B* **2003**, *107*, 7343.
(21) Haynes, C. L.; McFarland, A. D.; Zhao, L.; Van Duyne, R. P.; Schatz, G. C.; Gunnarsson, L.; Prikulis, J.; Kasemo, B.; Kaell, M. *J. Phys. Chem. B* **2003**, *107*, 7337.
(22) Gunnarsson, L.; Rindzevicius, T.; Prikulis, J.; Kasemo, B.; Kaell, M.; Zou, S.; Schatz, G. C. *J. Phys. Chem. B* **2005**, *109*, 1079.
(23) Oldenburg, S. J.; Westcott, S. L.; Averitt, R. D.; Halas, N. J. *J. Chem. Phys.* **1999**, *111*, 4729.
(24) Link, S. E.-S., M. A. *J. Phys. Chem. B* **1999**, *103*, 8410.
(25) Sau, T. K.; Murphy, C. J. *Langmuir* **2004**, *20*, 6414.
(26) Payne, E. K.; Shuford, K. L.; Park, S.; Schatz, G. C.; Mirkin, C. A. *J. Phys. Chem. B* **2006**, *110*, 2150.
(27) Yonzon, C. R.; Stuart, D. A.; Zhang, X.; McFarland, A. D.; Haynes, C. L.; Van Duyne, R. P. *Talanta* **2005**, *67*, 438.
(28) Shaikh, K. A.; Ryu, K. S.; Goluch, E. D.; Nam, J.-M.; Liu, J.; Thaxton, C. S.; Chiesl, T. N.; Barron, A. E.; Lu, Y.; Mirkin, C. A.; Liu, C. *Proc. Natl. Acad. Sci. U.S.A.* **2005**, *102*, 9745.
(29) Haynes, C. L.; Yonzon, C. R.; Zhang, X.; Van Duyne, R. P. *J. Raman Spectrosc.* **2005**, *36*, 471.
(30) Cao, Y. C.; Jin, R.; Mirkin, C. A. *Science* **2002**, *297*, 1536.
(31) Zhang, X.; Young Matthew, A.; Lyandres, O.; Van Duyne Richard, P. *J. Am. Chem. Soc.* **2005**, *127*, 4484.
(32) Nath, N. C. A. *Anal. Chem.* **2002**, *74*, 504.
(33) Okamoto, T. Y., I.; Kobayashi, T. *Opt. Lett.* **2000**, *25*, 372.
(34) Hilger, A. C., N.; Tenfelde, M.; Kreibig, U. *Eur. Phys. J.* **2000**, *10*, 115.
(35) Henglein, A. M., D. *J. Phys. Chem. B* **1998**, *102*, 8364.
(36) Taton, T. A. L., G.; Mirkin, C. A. *J. Am. Chem. Soc.* **2001**, *123*, 5164.
(37) Schultz, S. S., D. R.; Mock, J. J.; Schultz, D. A. *Proc. Natl. Acad. Sci. U.S.A.* **2000**, *97*, 996.
(38) Sonnichsen, C. F., T.; Wilk, T.; von Plessen, G.; Feldmann,; J.; Wilson, O. M. P. *Phys. Rev. Lett.* **2002**, *88*, 077402/1.
(39) Connolly, S. C., S.; Fitzmaurice, D. *J. Phys. Chem. B* **2001**, *105*, 2222.
(40) Elghanian, R. S., J. J.; Mucic, R. C.; Letsinger, R. L.; Mirkin, C. A. *Science* **1997**, *227*, 1078.
(41) Mirkin, C. A. L., R. L.; Mucic, R. C.; Storhoff, J. J. *Nature* **1996**, *382*, 607.
(42) Storhoff, J. J. E. R.; Mucic, R. C.; Mirkin, C. A.; Letsinger, L. R. *J. Am. Chem. Soc.* **1998**, *120*, 1959.
(43) Miller, M. M.; Lazarides, A. A. *J. Phys. Chem. B* **2005**, *109*, 21556.
(44) Draine, B. T.; Flatau, P. J. *User Guide for the Discrete Dipole Approximation Code DDSCAT.6.0*. 2003, http://arxiv.org/abs/astro-ph/0309069.
(45) Haes, A. J.; Zou, S.; Schatz, G. C.; Van Duyne, R. P. *J. Phys. Chem. B* **2004**, *108*, 109.
(46) Haes, A. J.; Zou, S.; Schatz, G. C.; Van Duyne, R. P. *J. Phys. Chem. B* **2004**, *108*, 6961.
(47) Malinsky, M. D.; Kelly, K. L.; Schatz, G. C.; Van Duyne, R. P. *J. Phys. Chem.* **2001**, *105*, 2343.
(48) Kreibig, U. V., M. *Optical Properties of Metal Clusters*; Springer: Berlin, 1995.
(49) Whitney, A. V.; Elam, J. W.; Zou, S.; Zinovev, A. V.; Stair, P. C.; Schatz, G. C.; Van Duyne, R. P. *J. Phys. Chem. B* **2005**, *109*, 20522.

NL061286U